Water Resources Management (2021) 35:2369–2384
https://doi.org/10.1007/s11269-021-02818-2

Optimal Design and Feature Selection by Genetic Algorithm for Emotional Artificial Neural Network (EANN) in Rainfall-Runoff Modeling

Amir Molajou[1] **· Vahid Nourani**[2,3] **· Abbas Afshar**[1] **· Mina Khosravi**[1] **· Adam Brysiewicz**[4]

Received: 16 September 2020 / Accepted: 21 March 2021/ Published online: 22 April 2021

Abstract

Rainfall-runoff (r-r) modeling at different time scales is considered as a significant issue in hydro-environmental planning. As a first hydrological implementation, for one-time-ahead r-r modeling of two watersheds with totally distinct climatic conditions, Genetic Algorithm (GA, as a global search technique) and Emotional Artificial Neural Network (EANN, as a new production of Artificial Intelligence (AI) based methods that simulated based on the brain neurophysiological structure) was combined. Determining the optimal architecture of AI-based networks is vital for increasing the accuracy of prediction by the network and also to reduce run-time. In the current study, GA has been implemented to choose the important features candidate as EANN input and automatically diagnose the optimal number of hidden nodes and hormones simultaneously. The acquired results indicated a better representation of the proposed hybrid GA-EANN model compared to the sole ANN and EANN. Numerical identification of obtained results revealed that the proposed hybrid GA-EANN model might enhance the better results than the EANN model up to 19% and 35% in terms of testing suitability criteria for Aji Chai and Murrumbidgee catchments, respectively.

Keywords Rainfall-runoff modeling · Emotional artificial neural network (EANN) · Genetic algorithm (GA) · Feature selection · Structure optimization

1 Introduction

The rainfall-runoff (r-r) process is one of the most important and complex phenomena in the hydrological cycle. This process involves the movement of raindrops in different states and, finally, runoff formation in natural or artificial canals. It is evident that many hydraulic and hydrologic engineering projects need to have an accurate estimation of the quantity and

✉ Amir Molajou
amolajou@yahoo.com

Extended author information available on the last page of the article

characteristics of runoff from rainfall. In other words, it can be said that the accurate simulation of the r-r process is a notable stage in the water supply administration; so, accurate models are required to simulate this phenomenon (Rezaie-Balf et al., 2017; Safari et al., 2020; Molajou et al., 2021; Adnan et al., 2021).

In general, there are two approaches in modeling hydrological phenomena: i) conceptual (white box models) and ii) systemic (black box models). The conceptual perspective in hydrological processes is partly based on physical mechanisms, and the modeling process usually depends on the catchment characteristics. In contrast, in the systematic approach (black box), the purpose of the model is to create a mapping between input and output data without considering the structure and physical laws governing the phenomenon process. Many scientists and experts in water resources argue that the black box approach overcomes many physical approach complexities. They believe that this approach is an effective solution for hydrological processes modeling (such as r-r modeling) because of complex abstruse and unknown parameters involved in these processes (Nayak et al. 2004; Sharghi et al., 2018a; Nourani et al., 2018).

One of the most famous and oldest systemic approach models is the Auto-Regressive Integrated Moving Average (ARIMA), which has been used in many studies to predict various hydrological processes. In this model, regardless of the physical structure of the phenomenon, a relationship is established in the form of a regression formula between input and output data. Although this approach leads to the creation of models that are basically linear in structure and are often used for static series, but nevertheless have a limited ability to model unstable series and phenomena of nonlinear nature. Therefore, to solve this problem, another group of black-box models based on artificial intelligence (AI) knowledge called artificial neural networks (ANNs) were developed.

In recent decades, ANN models, which are identified as a self-learning method, have been broadly utilized for simulating non-linear hydrological time series. The ANN can apply high order equations to handle the non-linear part of the process, and it has the capacity to examine multivariate information with complex components with no obligation of former knowledge about the practice (Nazif et al., 2009; Nourani et al. 2019a; Sharghi et al., 2021). Due to the unique features of ANN-based models, in recent decades, these models have been successfully used in various fields of hydrological processes, including r-r modeling (e.g., see ASCE 2000; Maier and Dandy 2000; Dawson and Wilby 2001; Jain and Srinivasulu 2006; Abrahart et al. 2012; Adamowski et al., 2012).

Despite the capabilities of ANN in time series modeling, sometimes due to the large fluctuations in the time series that cause its instability, there are problems in modeling with this method. Under such conditions, the ANN models are not able to properly model unstable time series without pre-processing the input and output time series data. To increase the ability of ANN to handle the seasonality characteristic of time series, a hybrid model via linking an appropriate pre-processing tool (e.g., wavelet transform) to AI-based models was proposed. The hybrid Wavelet-ANN model (WANN) is a well-designed organization that appropriates the wavelet change to get separate incidences of the r-r process and calculate the expected runoff at the aspired range by ANN. Regardless of the appropriate performance of the hybrid WANN model in r-r modeling, some weaknesses can be mentioned for this hybrid model. One of these weaknesses is that such data-processing devices should be done within an outside unit disassociated from ANN models' structure (Sharghi et al., 2018a; Nourani et al., 2019b).

In recent years, a new family of ANN models combining artificial emotions in the classic ANN framework has been introduced as emotional ANN models (EANNs). Biologically, animals' neurophysiological responses can be affected by hormonal activity so that animals may offer different actions for the same task in different moods (Khashman, 2008; Lotfi and Akbarzadeh, 2014 and 2016; Nourani et al., 2019b). Inspired by this biological concept that integrates artificial emotions and ANN, network learning ability can be enhanced due to the feedback loop between hormone systems and nerve cells (Kumar et al., 2019; Yaseen et al., 2020; Temeng et al., 2020).

The generalization ability of ANN-based models, which is the process of learning the relationship between the training dataset and handling the unseen test data, has made it a popular tool that is applied in different fields by researchers. Besides the generalization ability, any function in a stable mode can be practically approximated by ANN. However, designing the structure of ANN-based models is a difficult task (including the number of hormones, the number of hidden nodes (HN), and adjustment of different factors (e.g., epoch number and connection weights)). Determination of HN and hormone size is the critical scheme issue in ANN/EANN structures. Less number of HN can be led to the under-fitting problem, while a large number of HN can result an over-fitted model (Over-fitting can cause efficient performance in the training stage but poor performance in the testing stage (Kermani et al., 1995)).

The selection of the appropriate feature subset is another significant factor affecting the efficiency of ANN/EANN. For a given task, all of the traits are not significant in the same way (i.e., some are Clamorous, irrelevant, and redundant). The generalization ability can be improved by choosing the appropriate point subset. The appropriate parameter selection of ANN/EANN structure can minimize the computational attempt of the training stage. It is noteworthy to mention that the optimal selection of input features (i.e., HN size and hormones) should be done automatically and simultaneously because the optimal amount of HN and hormones are extremely dependent on the number of input characteristics. However, irrelevant and redundant information may be involved in input features. To improve the generalization ability, removing irrelevant and redundant information is an essential step. Therefore, the required number of HN would be changed, as well. In this case, the utilization of the Genetic Algorithm (GA) would be a promising alternative in multi-parameter optimization (Ahmad et al., 2010; Rohani et al., 2015).

In the current study, as a novel strategy, the new hybrid GA-EANN model (GA coupled with EANN model) for r-r modeling is introduced. In the proposed model, GA has the ability to determine the optimal structure of the network (selecting the significant features of inputs and determining the optimal number of HN and hormones), and EANN is capable of recognizing and distinguishing rainy and rainless days via the hormonal parameters of the artificial emotional system. It should be noted that this is the first research and usage of the proposed hybrid GA-EANN model in hydrologic engineering.

2 Materials and Methods

2.1 Emotional Artificial Neural Network (EANN)

To manage the multiple and non-linear aspects of hydrological time series, non-linear AI-based models, notably ANN, have been extensively executed to compose useful connections among input and output datasets. Consequently, utilization of ANN as an

AI-based approach has been examined at distinct fields of science due to its exceptional benefits such as i) no provision of earlier knowledge, ii) training a non-linear system, and iii) the capability of examining the multivariate output/inputs with various features (Nourani et al., 2019b).

The novel comparisons told that Feed-Forward Neural Network (FFNN), as the first generation of ANN-based models, with backpropagation (BP) algorithm, can have relatively reliable results in the modeling of nonlinear hydro-environmental variables (ASCE, 2000).

From different perspectives, the role of emotions in AI (like as agents interact with humans, systems apply the emotions to assist their own logic or creation of agents that more similar to human emotional behaviors) have been studied by researchers (Lewin 2001). Contrary to humans, computers do not benefit from physiologies like regulatory signals and information circulate within them. As a biological attitude, the neurophysiological reaction of the animal can be affected by animal conditions due to the secretion of hormone glands. It may sometimes show different reactions for an analogous function (or role) at different moods. In a similar way, for an EANN model, there will be a feedback ring within the hormonal and neural operations (Yaseen et al., 2020).

To enhance the BP learning algorithm of the multi-layer perceptron systems, nervous anxiety, and belief, administrators are concerned. According to the template of the information example, the anxiety factor is initialized for per education example in the recommended Emotional Back Propagation (EmBP) network. The algorithm is adjusted within the instruction repetition. Contrariwise, the resolution factor is related to the stress portion, and this arrangement production at the first emphasis. The spirit and anxiety levels are sequentially low and high at the opening of a training phase, and they are going to be developed and settled sequentially after a few thriving training emphases. Inside the preparation rule of EmBP, the error pitch in the network's output would hurt from less concentration if a high value was attached to the stress portion. Yet, the resolution circumstance increase (due to force discount) overcomes the network to return more awareness to the weights shift in the former practice tread. In fact, this process is similar to increase the inertia term to moderate the alteration degree from a pattern to the other as the learning emphasis has proceeded. From the measurable perspective, an EANN involves a few additional factors that are dynamically socialized with data, products, and mathematical weights of the network with regard to classic ANN (see Fig. 1).

In each hidden neuron of the EANN model, the learning recurrently converts among facts and production systems (as can be seen in Fig. 1). These neurons also give dynamical hormones of H_c, H_b, and H_a, which they are primarily identified based on the production and data rates and then are produced within the learning process in the preparation degree of the model. The hormonal coefficients influence other neurons' units in the education manner (as shown in Fig. 1). The neural and hormonal routes of the information are dispensed by dotted and solid lines in Fig. 2. Through the EANN model, the data of the i^{th} node with three hormones of H_c, H_b, and H_a is considered as (Nourani et al., 2019b):

$$Y_i = \underbrace{(\gamma_i + \sum_h \partial_{i,h} H_h)}_{1} \times f(\sum_j [\underbrace{(\beta_i + \sum_h \chi_{i,h} H_h)}_{2} \times \underbrace{(\alpha_{i,j} + \sum_h \Phi_{i,j,k} H_h) X_{i,j}}_{3}) + \underbrace{(\mu_i + \sum_h \psi_{i,h} H_h)]}_{4})$$

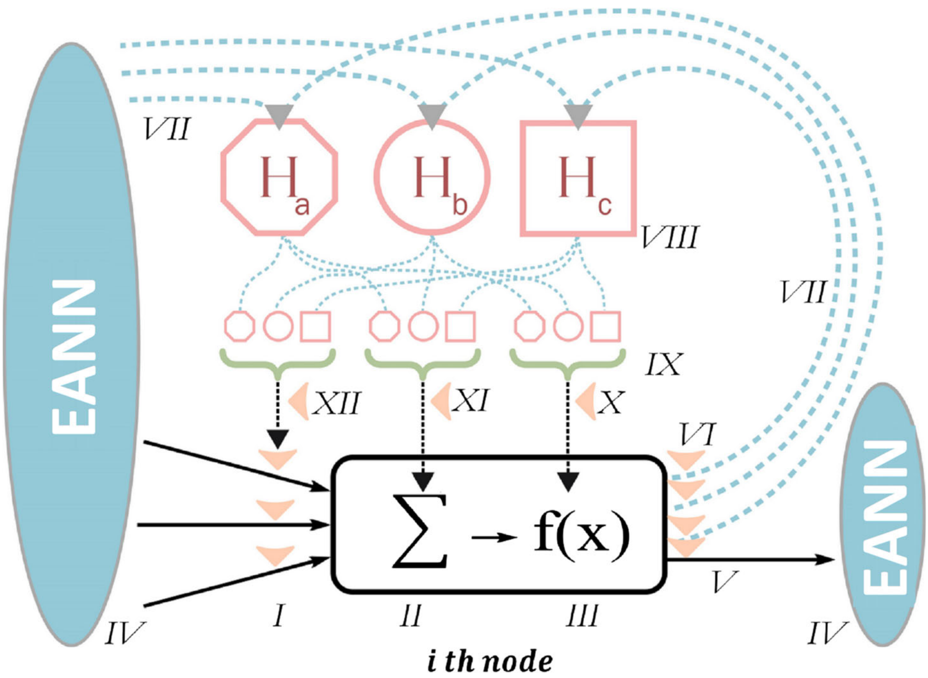

Fig. 1 The emotional unit and EANN node (Sharghi et al., 2018a,b)

As the artificial hormones calculated as:

$$H_h = \sum_i H_{i.h} \qquad (h = a, b, c) \tag{2}$$

In relation 1, the implemented weight to the goal (*f*) is depicted by (1). It incorporates the permanent neural influence such as the dynamic hormonal weight of $\sum_h \partial_{i,h} H_h$. The implemented weight to the gathering (net) function is given by Term (2), the employed weight to the $X_{i,j}$ (an input from *j* the node of the former layer) is confirmed by Term (3), and the preference of the summation purpose is indicated by Term (4).

The distribution of the overall hormonal level of EANN (i.e., H_h) between the hormones must be verified by, and circumstances, the i th node output (Y_i) provide hormonal feedback of $H_{i,h}$ to the network as follows (Sharghi et al., 2018a,b):

$$H_{i,h} = glandity_{i,h} \times Y_i \tag{3}$$

Where the *glandity* parameter can be calibrated in the training phase of the EANN model to find the appropriate hormone size for the glands.

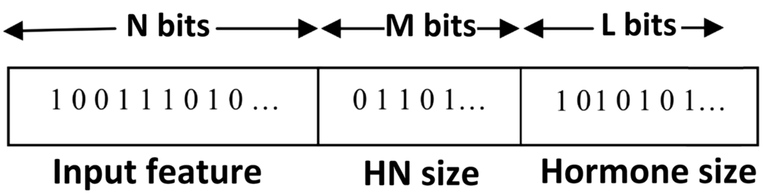

Fig. 2 Binary coded GA representation

2.2 Genetic Algorithm (GA)

In the field of soft computing, global search heuristics contains various techniques. One of the most commonly used techniques among researchers is GA. By making use of techniques that are inspired by evolutionary biology processes (such as mutation, crossover, inheritance, and selection), GA is categorized as an evolutionary algorithm (Xiao et al., 2009; Ahmad et al., 2010).

As shown in Fig. 2, in the GA algorithm, parameters are collected in chromosomes containing three parts: features, nodes, and hormones. It should be noted to represent the chromosomes; binary code GA is utilized. The first part, feature, contains N bits which indicate the N number of features of the dataset. To illustrate the feature at a certain location that is selected or not, value "0" indicates "not selected," and value "1" means "selected." The second part, node, consists of M bits which represent the M number of nodes at the EANN hidden layer. Automatically the length of chromosomes length is set so that a similar decimal price is equal to or more than the double of the first part (feature number). It is obvious that the maximum number of HN size is 2^M because of the M binary bits of the nodes. And the last part signifies the L number of hormones contained in the chromosome at EANN. The reason for this presentation's preference over others is whether the network size is big or small; it requires a small code (Ahmad et al., 2010).

Mean Square Error (MSE) of the validation dataset as confirmed in (Eq. 4), is the foundation of the shape function calculation, where q is the number of separate data sets (examples), p intimates the number of crop nodes, is objective value of m^{th} output node for nth design and is the output value of nth node for mth ornament (Ahmad et al., 2010).

$$\mathrm{MSE} = \frac{100}{pq} \times \sum_{m=1}^{p} \sum_{n=1}^{q} \left(O_m^n - T_m^n\right)^2 \tag{4}$$

For next-generation, chromosomes should mate and survive. So, to be selected as a parent, chromosomes with lower MSE have a higher chance among others. The first step of the selection process is transforming the MSE value to its ranking. The higher ranks indicate the considered chromosome is better than the others. At the next step, based on the ranking that the m^{th} chromosome has got, its fitness will be calculated.

$$fitness\ (m) = \frac{rank\ (m) \times 100}{\sum_{n=1}^{m} rank\ (n)} \tag{5}$$

And then, to choose which pair of chromosomes will be the parents, roulette-wheel selection is utilized, based on the chromosome's ranks. After defining the parent chromosomes, a crossover operation will happen. By the crossover process, two new children will be produced with genetic information which is inherited from their parent chromosomes. These two new chromosomes will replace the last pair of chromosomes with the lowest ranks. This is an emulation of a bio-evolution process in which the worst (low-rank) chromosomes die and are replaced by new chromosomes, while the chromosomes with suitable fitness will survive and move to the next generation. And the last step of these processes is the mutation which all the chromosomes will transpire into. In this study, modification operation and standard single-point crossover are employed. In each generation's crossover operation process, only the pair of chromosomes with the highest ranks (parent) will be selected to operate. Generating an unmethodical crossover point is the first step of the crossover operation process. Then, all bits after the generated point will exchange among the parent chromosomes to produce two new chromosomes. Afterward, the two newborn chromosomes will replace the lowest rank chromosomes. Later on, the mutation process will be performed on all the chromosomes. Based on the mutation likelihood, every bit of the chromosome will switch between two modes, 'selected' or 'not selected' (i.e., '0' or '1') (Ahmad et al., 2010).

2.3 Proficiency Criteria

The proficiency of the models was assessed by the mean square error (MSE) as:

$$MSE = \frac{\sum_{i=1}^{N}\left(Q-\widehat{Q}_i\right)^2}{N} \tag{6}$$

Where N, Q_i and $\widehat{Q}_i$ are the number of observations, observed, and calculated runoff values, respectively.

3 Results and Discussion

3.1 Two Distinct Watersheds

This research was surveyed on two watersheds, Aji Chai (Vanyar) and Murrumbidgee (Lobbs Hole Creek). The first one is placed in Iran, and another one is located in Australia. Surveys showed that the hydrological features of the catchments are totally different. The rainfall and runoff time series related to Aji Chai catchment show a distinct behavior (has seasonality and a regular pattern), but the time series of the Murrumbidgee catchment has a wild behavior (an irregular pattern). These catchments, with distinct and different climatic conditions, were selected to evaluate and compare the performance of the proposed hybris GA-EANN model.

The Lake Urmia watershed is placed in the North-Western of Iran and encompasses an area of 51.800 km^2. It is located at the longitudes of 44.14°E and 47.53°E and latitudes of 35.40$^o N$ and 38.20$^o N$. The lake catchment includes 14 main sub-basins surrounding the lake, with areas ranging from 431 to 11,759 km^2. There are many great and tiny streams in this container within 20 to 60 km long, among which the most prominent waterways are Zarrineh-Roud, Simineh-Roud, and Aji Chai. The Aji Chai catchment is an endorheic watershed that sheds into Urmia Lake (Fig. 3).

The climate of the Aji Chai catchment area is generally midcontinental. In other words, the study area has cold winters and relatively mild summers. The variety of air masses that affect this region is very diverse, and in different seasons of the year, the amount of precipitation and temperature of the region is very different. The average annual precipitation in the study basin varies from 300 to 700 mm, and its predominant regime is the Mediterranean, with little summer precipitation. In the current study, the daily runoff and rainfall time series of 22 years (from 1996 till 2017, 8030 days) were available and obtained from the Water and Sewage Company of East Azarbaijan province. The statistics of the observed daily time series (temperature, rainfall, and runoff) for the Vanyar watershed are reported in Table 1.

According to Fig. 4, the other studied watershed is the Lobbs Hole Creek. As shown in Fig. 5, the Lobbs Hole Creek is one of the main branches of the Murrumbidgee River that flows to the south of the Australian Capital Territory at New South Wales state (located at 35.54°S;

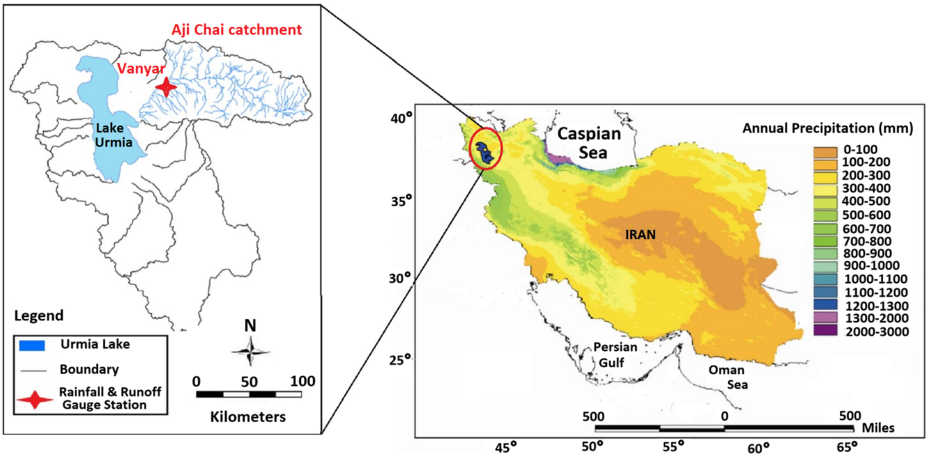

Fig. 3 The location of the Aji Chai catchment

149.11°E). The average amount of the watershed elevation is about 731 m above sea level, and it should be noted that the minimum watershed elevation is 586 m, and the maximum amount is 1870 m. Another point to note is that grass (12%) and trees (88%) are the dominant vegetation types of the watershed and the population density of the river area is about four people/km^2, and that is why it can be said human activities do not influence the environment of the watershed. The watershed has a cool-temperature seaside atmosphere with a medium heat of 14 °C. Sequentially, January and July are the most heated and coolest months with common temperatures of 24 °C and 4 °C. Another important issue to note is that the rainfall is almost uniformly distributed over the year, but only a few days of winter, this area is faced with falling snow. July and February are the most dry and wet months of the year, with average rainfall values of about 35 mm and about 164 mm, respectively. Twenty-two years of daily runoff and rainfall data (from 1996 till 2017, 8030 days) measured in Ainslie Tyson station near the hydrometric station were retrieved via the www.bom.gov.au/water/hrs website. The statistics of the synoptic data include rainfall and temperature, have been arranged in Table 2.

Table 1 The daily statistics of the temperature, rainfall, and runoff time series for the Vanyar watershed

Time Scale	Statistical period	Time-Series	Statistical factors	
Daily	1996–2017	Temperature (°C)	Min	−21.3
			Max	39.2
			Mean	10.49
			*S.D.	13.64
		Rainfall (mm)	Min	0
			Max	37
			Mean	0.67
			*S. D.	2.39
		Runoff (CMS**)	Min	0
			Max	190
			Mean	8.39
			*S. D.	16.69

*S. D.: Standard Deviation; ** Cubic Meter per Second (m^3/s)

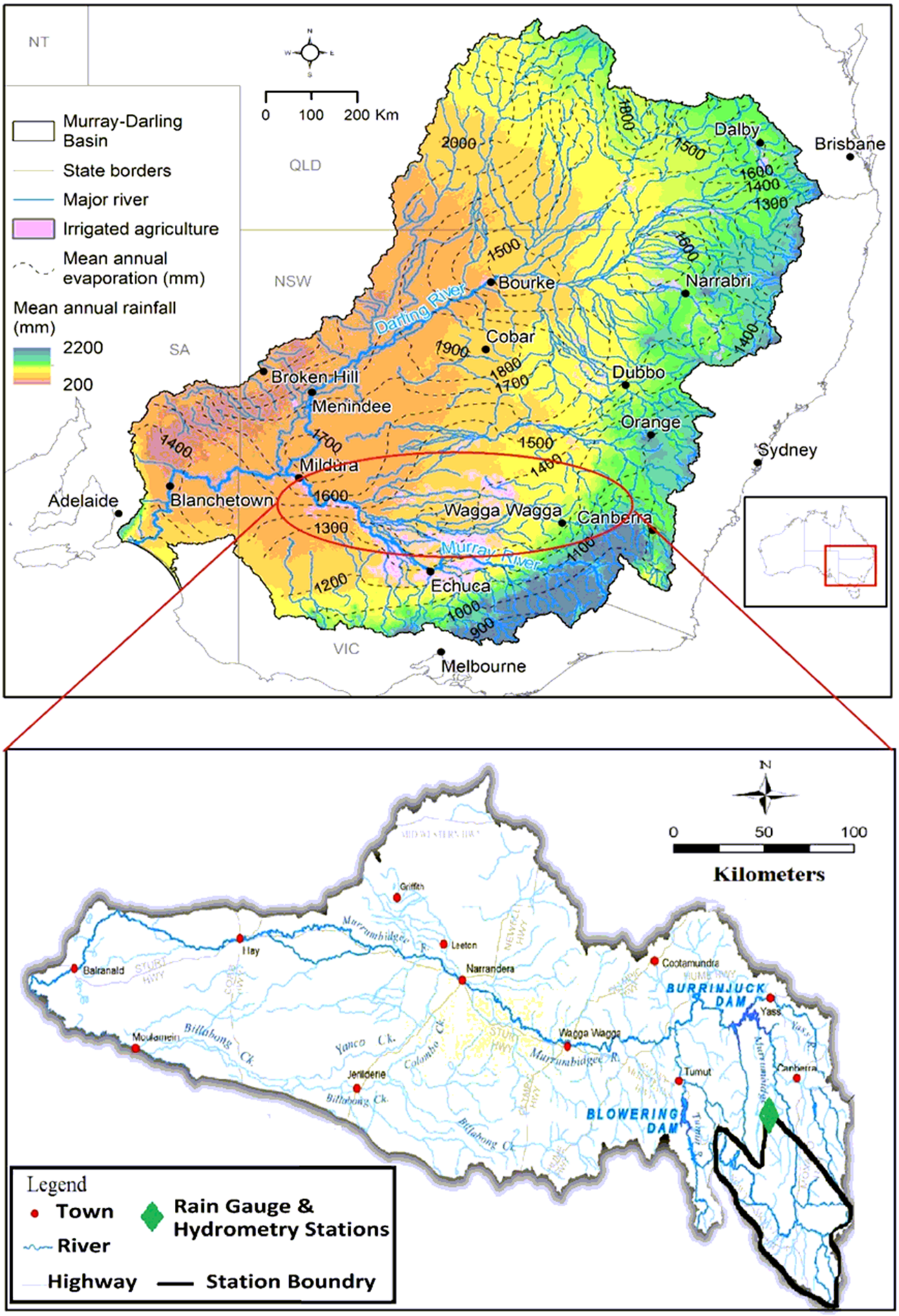

Fig. 4 The location of the Murrumbidgee catchment

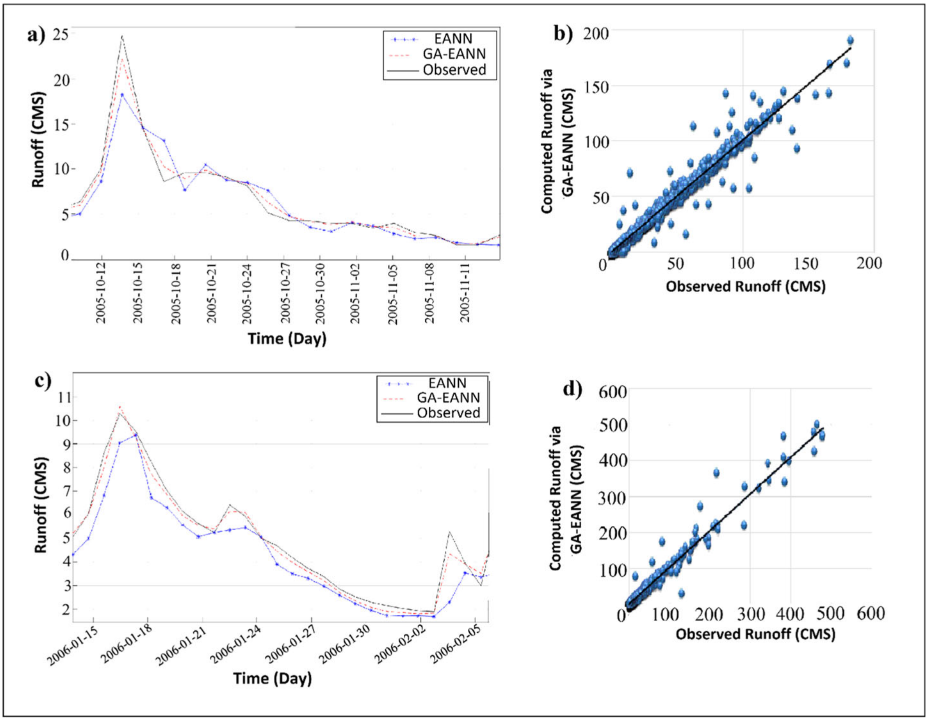

Fig. 5 Computed versus observed runoff at daily time scale for a,b) Vanyar and c,d) Lobbs Hole Creek

With the precision in the S.D. values of the daily statistics of rainfall and runoff time series (Tables 1 and 2) for the Vanyar and Lobbs Hole Creek watersheds, it can be resulted that the Lobbs Hole Creek watersheds' runoff and rainfall data are scattered more than the Vanyar watershed. Also, as shown in Tables 1 and 2, the S.D. values of the Vanyar watershed data are close to 0 compared to Lobbs Hole Creek data. It indicates that the data were closer to the mean value with a little dispersion (most rainfall and runoff values were about 0). The difference of data dispersion besides the correlation coefficient values for the runoff and rainfall can justify the difference in the catchments' behavior. Vanyar watershed follows a regular pattern and linear behavior, thus can be considered as a well-dominated seasonal catchment, while Lobbs Hole Creek watershed follows the irregular and non-linear pattern as a wild basin.

3.2 Verification of the Proposed Method

The importance of the many agents such as rainfall, evapotranspiration, trees, etc., are contained in the r-r procedure; hence, the passage of the most useful factors as information variables is a dominant stage for the r-r modeling. Former investigations noted that the r-r rule is named as a Markovian or autoregressive manner (its immediate amount has the closest relation with its previous amounts). Consequently, the fashionable river secretion will be a function of forerunner rainfall up to future stage m and flow up to present rest n senses, as:

Table 2 The daily statistics of the temperature, rainfall, and runoff time series for the Lobbs Hole Creek watershed

Time Scale	Statistical period	Time-Series	Statistical factors	
Daily	1996–2017	Temperature (°C)	Min	−6.3
			Max	45.6
			Mean	14.47
			*S.D.	12.39
		Rainfall (mm)	Min	0
			Max	100
			Mean	1.84
			*S. D.	6.07
		Runoff (CMS**)	Min	0
			Max	499.39
			Mean	5.83
			*S. D.	20.25

* S. D.: Standard Deviation; ** Cubic Meter per Second (m^3 /s)

$$Q_t = f(Q_{t-1}, Q_{t-2}, \ldots, Q_{t-n}, I_{t-1}, I_{t-2}, \ldots, I_{t-m}) \tag{7}$$

The earlier studies have emphasized that the period number for the model training in classic ANN models is extremely linked to the management of the runoff immune. Taking the examples, the behavior pattern is totally distinctive. This distinction can be hand in testifying the obtained results. By precise consideration is paid to Vanyar, the watershed experiences well-dominated annual drought. This causes its behavior approaches to semi-linear behavior. It might be supposed that due to the larger area of the Lobbs Hole Creek, the basin shows linear performance because the basin itself works as a chill and diminishes the variations of the runoff time series. But it can be figured out that the consequence of the irregular rainfall is more aggressive than the factor of breadth, and therefore it may cause more important non-linear behavior.

As mentioned in the introduction segment, defining the optimal architecture of the system, i.e., the number of protected neurons, hormones, and best practice period figure, have crucial tasks in FFNN and EANN instruction means, and their suitable election can limit over-learning of the network. In this comparison, for FFNN and EANN images, the tangent sigmoid and pure line was apiece considered for activation functions of the hidden and output layers, and this choice construction and stress epoch number networks were purchased via the trial-error manner (see Table 3).

As can be seen in Table 3, in both watersheds, the EANN has better efficiency than the FFNN. The most important point which can be derived from the one-step-ahead predicting of the EANN model efficiency is its performance with regard to the non-stationary nature of the input time series of the r-r process. EANN can overcome both autoregressive (Markovian) and seasonal properties of the process; therefore, EANN indicated high efficiency. Also, like previous studies, the results indicated that the EANN model can accurately capture the signal features, particularly peak values, and obtained comparatively acceptable performance, while the FFNN model cannot overcome the under/overestimation of the peak values.

As a unique strategy, in the contemporary study, GA has been utilized to select significant features as data to EANN simultaneously. The GA parameters are the community size (15), crossover promise, and mutation probability (0.15). The 8030 daily data for two watersheds are broken into ten sub-datasets; first, three sub-data collections comprise 810 data, and the left contains 800 data. This is to assure that all the information is used at least once for training,

Table 3 FFNN and EANN simulation for two watersheds

Watershed	Model	Input	No. of HN	No. of hormone	MSE (normalized)		
					Train	Validation	Test
Vanyar	FFNN	Q_{t-1}, Q_{t-2}, Q_{t-3}, I_{t-1}	7	0	0.013	0.014	0.023
	EANN	Q_{t-1}, Q_{t-2}, Q_{t-3}, I_{t-1}	3	2	0.008	0.010	0.013
Lobbs Hole Creek	FFNN	Q_{t-1}, Q_{t-2}, I_{t-1}	9	0	0.019	0.027	0.041
	EANN	Q_{t-1}, Q_{t-2}, I_{t-1}	4	4	0.029	0.018	0.027

validation, and verification. While the complete evaluation is a concern, the ten-fold cross-validation design is readjusted. The results of the proposed model (GA-EANN) are reported in Tables 4 and 5 for the case studies.

As can be seen from the results presented in Tables 4 and 5, the most important GA selected feature for both watersheds is $Q(t-1)$ so that the average GA selected features of Q(t-1) for Vanyar and Lobbs Hole Creek watersheds are 0.8 and 0.9, respectively. Also, by looking closely at the results, it can be seen that the GA selected the number of hormones and HN for the Vanyar watershed is greater than the Lobbs Hole Creek watershed in mostly data partition. This seems to be due to wild behavior (which has an irregular pattern) of Lobbs Hole Creek watershed compared with distinct behavior (which has seasonality and a regular pattern) of Vanyar watershed. As mentioned in the “Two Distinct Watersheds” section, the behavior pattern of the selected case studies (Vanyar and Lobbs Hole Creek watersheds) is totally different. The identifying of this basic difference of the watersheds’ behavior can be useful in the explanation of the observed results. If more individual attention is spent on the Vanyar watershed, it is recognized that this watershed experiences well-dominated seasonal weather, which led to semi-linear behavior. Maybe, it is assumed that this large basin shows linear behavior because of the greater area of the Lobbs Hole Creek watershed. But it can be understood that the irregular rainfall’s influence is more dominant than the parameter of breadth, and therefore it may cause higher non-linear behavior. For this reason, as can be seen in Tables 4 and 5, the HN size and Hormone size for Lobbs Hole Creek watershed are larger than the Vanyar watershed.

Table 4 GA selected feature, HN size, and hormone number for Vanyar watershed

Data partition	GA selected feature								GA selected No. of hormone	GA selected No. of HN	MSE (normalized)		
	I_{t-4}	I_{t-3}	I_{t-2}	I_{t-1}	Q_{t-4}	Q_{t-3}	Q_{t-2}	Q_{t-1}			Train	Validation	Test
1–5,6-9,10	0	1	0	1	0	1	1	0	4	4	0.011	0.014	0.017
2–6,7-10,1	0	0	1	0	0	0	1	1	1	5	0.003	0.009	0.010
3–7,8-1,2	0	1	0	1	0	0	1	1	2	3	0.010	0.008	0.016
4–8,9-2,3	0	0	0	0	0	1	1	0	3	3	0.009	0.013	0.008
5–9,10-3,4	1	0	1	0	1	1	0	1	3	4	0.008	0.006	0.013
6–10,1-4,5	0	0	0	1	0	1	1	1	1	3	0.009	0.010	0.013
7–1,2-5,6	0	0	1	1	1	1	0	1	2	2	0.006	0.011	0.008
8–2,3-6,7	0	0	0	1	0	0	1	1	0	3	0.002	0.003	0.009
9–3,4-7,8	0	0	0	0	0	1	1	1	0	2	0.001	0.003	0.003
10–4,5-8,9	0	1	0	1	1	1	1	1	3	3	0.009	0.009	0.012
Average	0.1	0.3	0.3	0.6	0.4	0.7	0.8	0.8	1.6	3.1	0.0068	0.0086	0.0109

Table 5 GA selected feature, HN size, and hormone number for Lobbs Hole Creek watershed

Data partition	GA selected feature								GA selected No. of hormone	GA selected No. of HN	MSE (normalized)		
	I_{t-4}	I_{t-3}	I_{t-2}	I_{t-1}	Q_{t-4}	Q_{t-3}	Q_{t-2}	Q_{t-1}			Train	Validation	Test
1–5,6-9,10	0	0	1	1	0	1	1	1	0	6	0.010	0.008	0.012
2–6,7-10,1	1	0	1	0	0	0	1	1	1	4	0.012	0.011	0.019
3–7,8-1,2	0	1	0	1	1	0	1	1	5	6	0.021	0.029	0.032
4–8,9-2,3	0	0	0	1	0	1	1	0	5	3	0.027	0.021	0.013
5–9,10-3,4	0	0	1	0	1	1	0	1	3	5	0.014	0.016	0.009
6–10,1-4,5	0	1	0	1	0	1	1	1	2	4	0.015	0.016	0.024
7–1,2-5,6	0	0	1	1	1	0	0	1	4	5	0.019	0.010	0.017
8–2,3-6,7	1	0	0	1	1	0	0	1	7	3	0.022	0.013	0.027
9–3,4-7,8	0	0	0	0	0	1	1	1	0	6	0.007	0.011	0.010
10–4,5-8,9	0	0	0	0	1	1	1	1	0	5	0.009	0.007	0.011
Average	0.2	0.2	0.4	0.6	0.5	0.6	0.7	0.9	2.7	4.7	0.0156	0.0142	0.0174

By comparing the results of Table 3 with the results of Tables 4 and 5, it can be said that the proposed GA-EANN model may enhance the better results than the EANN model up to 19% and 35% in terms of testing suitability criteria for Vanyar and Lobbs Hole Creek watersheds, respectively. To better compare the proposed GA-EANN model's performance with the EANN model, a part of the calculated time series by these models versus the observed time series is presented in Fig. 5.

Previous studies have all emphasized the high efficiency of the EANN model in different time series modeling (Sharghi et al., 2018a; Nourani et al., 2019b; Yaseen et al., 2020). However, due to the fact that achieving the optimal structure of this model using the trial and error method requires a lot of time, in the current study, it was shown that using the proposed GA-EANN model, in addition to reducing run-time, also improved the model results (see Fig. 5). As it can be seen in Fig. 5, the proposed hybrid GA-EANN, due to benefiting of the GA and EANN, in much less time can handle both seasonal and Markovian features of the r-r procedure, and it can accurately capture the signal properties especially peak values and obtained comparatively high performance. Most importantly, there is no need for trial and error, and the most optimal and accurate EANN structure can provide excellent results.

4 Conclusions

Determining the optimal architecture of neural networks (including the number of inputs, number of hidden layers, number of neurons in each hidden layer, transmission function of each layer, and number of hormones) plays a decisive role in increasing the accuracy of prediction by the network. Previous studies have often used trial and error to determine the optimal architecture of neural networks. Obviously, this method is time-consuming and therefore increases the computational costs. It can also be pointed out that this method is not accurate enough.

As a novel strategy, in the current study, it was tried to introduce a new composite representation to reach optimal design and background choice by GA for EANN (as a new production of AI-based model). In the first step, automatic feature selection and determination of essential parameters (HN and hormone size) based on GA-EANN hybrid intelligence is applied to detect the feature importance. Based on the feature importance, a series of feature subsets is manually created, and the EANN is retrained using this subset. The approach, which is based on a simple binary-coded GA representation, has overcome the tedious trial and error design process of EANN, especially in determining the HN and hormone size and the selection of significant features.

The proposed hybrid GA-EANN model is implemented to model the r-r procedure for two diverse catchments with totally distinct climatic conditions. The outcomes proved that utilizing the characteristic selection in the EANN classifier increased the accuracy of the classification process and, at the same time, reduced the network complexity. Also, the results showed the high efficiency of the hybrid GA-EANN compared to the sole EANN and FFNN models. Digital identification of the obtained results revealed that the suggested hybrid GA-EANN model might function more beneficial than the EANN model up to 19% and 35% in terms of testing response criteria for Aji Chai and Murrumbidgee catchments, sequentially.

Such a strong display of GA-EANN in r-r modeling can be suggested to simulate the other hydrological procedures. Taking the scientific forecasting, the mentioned hybrid GA-EANN model could be applied to build advanced collection prophecies at added front increments.

Availability of Data and Material Not applicable.

Code availability. Not applicable.

Authors' Contributions Amir Molajou: Conceptualization, Code Developer, Formal analysis, Writing - original draft.

Vahid Nourani: Supervision, Methodology, Review & Editing.

Abbas Afshar: Supervision, Methodology, Review & Editing.

Mina Khosravi: Formal analysis, Writing - original draft, Visualization.

Adam Brysiewicz: Visualization; Original draft; Review & Editing.

The authors give their full consent for the publication of this manuscript.

Declarations

Ethics Approval Not applicable.

Consent to Participate Not applicable.

Conflicts of Interest/Competing Interests None.

References

Abrahart RJ, Anctil F, Coulibaly P, Dawson CW, Mount NJ, See LM, Shamseldin AY, Solomatine DP, Toth E, Wilby RL (2012) Two decades of anarchy? Emerging themes and outstanding challenges for neural network river forecasting. Prog Phys Geograph. 36(4):480–513

Adamowski J, Chan E, Prasher S, Ozga-Zielinski B, Sliusareva A (2012) Comparison of multiple linear and non-linear regression, autoregressive integrated moving average, artificial neural network, and wavelet artificial neural network methods for urban water demand forecasting in Montreal, Canada. Water Res Res. 48(1). https://doi.org/10.1029/2010WR009945

Adnan RM, Petroselli A, Heddam S, Santos CAG, Kisi O (2021) Comparison of different methodologies for rainfall–runoff modeling: machine learning vs conceptual approach. Natural Hazards *105*(3):2987–3011

Ahmad F, Mat-Isa NA, Hussain Z, Boudville R, Osman MK (2010) Genetic algorithm - artificial neural network (GA-ANN) hybrid intelligence for cancer diagnosis. Second International Conference on Computational Intelligence, Communication Systems and Networks

ASCE Task Committee on application of Artificial Neural Networks in Hydrology (2000) Artificial neural networks in hydrology. II: Hydrologic applications. J Hydrol Eng. **5**(2):124–137

Dawson C, Wilby R (2001) Hydrological modelling using artificial neural networks. Prog Phys Geograph. **25**(1): 80–108

Jain A, Srinivasulu S (2006) Integrated approach to model decomposed flow hydrograph using artificial neural network and conceptual techniques. J Hydrol. **317**(3):291–306

Kermani BG, White MW, Nagle HT (1995) Feature extraction by genetic algorithms for neural networks in breast cancer classification, Engineering in Medicine and Biology Society, IEEE 17th Annual Conference

Khashman A (2008) A modified backpropagation learning algorithm with added emtional coeeficent. IEEE Trans Neural Netw Learn Syst. 19:1896–1909

Kumar S, Roshni T, Himayoun D (2019) A comparison of emotional neural network (ENN) and artificial neural network (ANN) approach for rainfall-runoff modelling. Civil Eng J *5*(10):2120–2130

Lewin DI (2001) Why is that computer laughing? IEEE Intell Systes. 16(5):79–81

Lotfi E, Akbarzadeh-T MR (2014) Practical emotional neural networks. Neural Netw. 59:61–72

Lotfi E, Akbarzadeh-T MR (2016) A winner-take-all approach to emotional neural networks with universal approximation property. Inf Sci. 347:369–388

Maier HR, Dandy GC (2000) Neural networks for the prediction and forecasting of water resources variables: a review of modelling issues and applications. Environ Modell Software. **15**(1):101–124

Molajou A, Afshar A, Khosravi M, Soleimanian E, Vahabzadeh M, Variani HA (2021) A new paradigm of water, food, and energy nexus. Environ Sci Pollut Res:1–11. https://doi.org/10.1007/s11356-021-13034-1

Nayak PC, Sudheer K, Rangan D, Ramasastri K (2004) A neuro-fuzzy computing technique for modeling hydrological time series. J Hydrol **291**(1):52–66

Nazif S, Karamouz M, Fallahi M, Rahimi M (2009) Long Lead Rainfall Prediction Using Statistical Downscaling and Articial Neural Network Modeling. Scientia Iranica 16(2):165–172

Nourani V, Davanlou Tajbakhsh A, Molajou A (2018) Data mining based on wavelet and decision tree for rainfall-runoff simulation. Hydrol Res. 50(1):75–84

Nourani V, Molajou A, Najafi H, Mehr AD (2019a) Emotional ANN (EANN): a new generation of neural networks for hydrological modeling in IoT. In Artificial Intelligence in IoT (pp. 45–61). Springer, Cham

Nourani V, Molajou A, Uzelaltinbulat S, Sadikoglu F (2019b) Emotional artificial neural networks (EANNs) for multi-step ahead prediction of monthly precipitation; case study: Northern Cyprus. Theoretic Appl Climatol 138(3):1419–1434

Rezaie-Balf M, Zahmatkesh Z, Kim S (2017) Soft computing techniques for rainfall-runoff simulation: local non–parametric paradigm vs. model classification methods. Water Res Manag *31*(12):3843–3865

Rohani M, Afshar MH, Moeini R (2015) Layout and Size Optimization of Sewer Networks by hybridizing the GHCA Model with Heuristic Algorithms. Scientia Iranica 22(6):2069–2082

Safari MJS, Arashloo SR, Mehr AD (2020) Rainfall-runoff modeling through regression in the reproducing kernel Hilbert space algorithm. J Hydrol *587*:125014

Sharghi E, Nourani V, Najafi H, Molajou A (2018a) Emotional ANN (EANN) and Wavelet-ANN (WANN) approaches for markovian and seasonal based modeling of rainfall-runoff process. Water Res Manag **32**(**10**): 3441–3456

Sharghi E, Nourani V, Molajou A, Najafi H (2018b) Conjunction of Emotional ANN (EANN) and wavelet transform for rainfall-runoff modeling. J hydroinform 21(1):136–152

Sharghi, E., Paknezhad, N. J., & Najafi, H. 2021. Assessing the effect of emotional unit of emotional ANN (EANN) in estimation of the prediction intervals of suspended sediment load modeling. *Earth Science Informatics*, 1–13

Temeng VA, Ziggah YY, Arthur CK (2020) A novel artificial intelligent model for predicting air overpressure using brain inspired emotional neural network. Int J Mining Sci Technol 30(5):683–689

Xiao, L., Wang Z. & Peng, X., 2009. Research on congestion control model and algorithm for high-speed network based on genetic neural network and intelligent PID, in Wireless Communications, Networking and Mobile Computing, 5th International Conference

Yaseen ZM, Naganna SR, Sa'adi Z, Samui P, Ghorbani MA, Salih SQ, Shahid S (2020) Hourly river flow forecasting: application of emotional neural network versus multiple machine learning paradigms. Water Res Manag *34*(3):1075–1091

Publisher's Note Springer Nature remains neutral with regard to jurisdictional claims in published maps and institutional affiliations.

Affiliations

Amir Molajou[1] **· Vahid Nourani**[2,3] **· Abbas Afshar**[1] **· Mina Khosravi**[1] **· Adam Brysiewicz**[4]

Vahid Nourani
vnourani@yahoo.com

Abbas Afshar
a_afshar@iust.ac.ir

Mina Khosravi
Mina.Khosravi1995@yahoo.com

Adam Brysiewicz
a.brysiewicz@itp.edu.pl

1 Department of Water Resources Eng., Faculty of Civil Eng, Iran University of Science & Technology, Tehran, Iran

2 Center of Excellence in Hydroinformatics and Faculty of Civil Engineering, University of Tabriz, Tabriz, Iran

3 Faculty of Civil and Environmental Engineering, Near East University, via Mersin 10, 99138 Nicosia, N Cyprus, Turkey

4 Institute of Technology and Life Sciences, Raszyn, Poland